35th Annual International Conference of the IEEE EMBS
Osaka, Japan, 3 - 7 July, 2013

Fabrication of Polymeric Microfluidic Devices with Tunable Wetting Behavior for Biomedical Applications*

Nicole E. Steidle[1], Marc Schneider[1], Ralf Ahrens[1], Matthias Worgull[1] and Andreas E. Guber[1]

***Abstract*— We demonstrate the fabrication of microchannels with specific fluidic behavior due to micro- and/or nanostructures on the surfaces. With a combination of hot embossing and microthermoforming it is possible to produce microchannels with specific surface properties. These surface properties are highly dependent on the micro- and nanostructures embossed into the material. Different structure sizes and geometries where examined by contact angle measurements. Here the dependency of diameter and pitch of the structures on the contact angle is examined as well as the material impact. These results enable the fabrication of highly specific surfaces tunable to an application.**

I. INTRODUCTION

Fabrication of polymeric microfluidic devices at low cost in high quantities with specific surface properties are eligible for many applications. Surface properties can be influenced by micro and nanostructures. They change wetting behavior [1], [2] and cell behavior [3], [4]. The effect of surface structures on the wetting behavior is also known from nature. The most famous representative is the lotus leaf. With the combination of hierarchical micro- and nanostructures and wax coatings it is possible to achieve high contact angles with low tilting angles thus enabling the self-cleaning effect of the lotus leaf [5]. Also high contact angles with high adhesion are used in nature like the rose petal [6]. The cell behavior can be influenced greatly by micro- and nanostructures. Yoon et al. discussed the passive control of cell locomotion, the cells movement and location, using micropatterns [3]. Other groups also examined the influence of surface structures to the cell adhesion or alignment [4]. However the fabrication of controlled structured surfaces for microfluidic devices is far from mass production.

In this work we introduce a combination of replication processes for the fabrication of microfluidic devices. The fabrication is divided into three steps: hot embossing, thermoforming and bonding. Hot embossing is a method used for the fabrication of micro- and nanostructures where high-precision manufacturing and precise control is needed [7]. Thermoforming or blow molding is a well-known method for the fabrication of three-dimensional shapes [8], [9]. By heating and introducing a gas pressure thermoplastic polymer foils are formed into a mold. Microscopic scale thermoforming is used for the fabrication of medical devices like miniature balloons [10]. In the bonding step we achieve a liquid-tight connection between the thermoformed polymer foil and a base plate, containing all the necessary fluidic connectors.

Because of the strong influence of the surface textures it is important to control surface structures and characterize the effect. This work also examined the influence of surface structures on the wetting behavior. Therefore contact angle measurements for four different materials with different structures were conducted to evaluate the influence of structure size, pitch and material on the wetting behavior.

This work shows a promising fabrication process to be capable of the mass production of low-cost surface-structured, biocompatible polymeric microfluidic devices for biomedical applications.

II. EXPERIMENTAL SETUP

The fabrication of microfluidic systems is a three step process. In the first process step foils with a thickness of 50 μm are structured with micro- and/or nanostructures. Afterwards these structured foils are brought into a three dimensional shape by thermoforming. In the last step the formed channel is bonded to a base plate with all the necessary connectors like fluid inlet and outlet. Fig. 1 shows a schematic view of the fabrication steps.

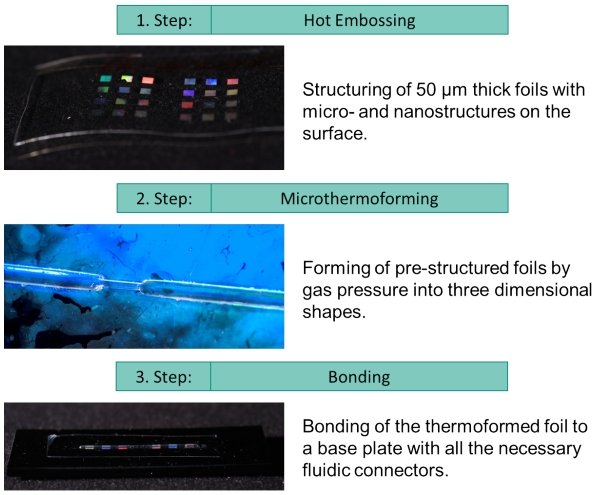

Fig. 1. Schematic view of the fabrication steps. In the first step a 50 μm thick foil is structured by hot embossing. This pre-structured foil is then brought into a three dimensional shape by microthermoforming. In the last step the thermoformed foil is bonded to a base plate with all the necessary fluidic connectors.

*Research supported by the Bürkert Technology Center (BTC), a cooperation between Bürkert GmbH & Co. KG and the Institute of Microstructure Technology (IMT) at the Karlsruhe Institute of Technology (KIT). This work was carried out with the support of the Karlsruhe Nano Micro Facility (KNMF, www.kit.edu/knmf), a Helmholtz Research Infrastructure at Karlsruhe Institute of Technology (KIT, www.kit.edu).

[1] All authors are with the Institute of Microstructure Technology, Karlsruhe Institute of Technology, Postfach 3640, 76021 Karlsruhe, Germany Nicole.steidle@kit.edu

A. Hot Embossing

Hot embossing is used for high-precision manufacturing of micro- and nanostructures. With hot embossing it is possible to fabricate structured thermoplastic polymer foils which can afterwards be used for thermoforming. In this work Polymethylmethacrylat (PMMA), Cyclic Olefin Copolymer (COC), Polycarbonate (PC) and Polysulfon (PSU) were chosen as materials due to their biocompatibility and therefore high usage in biological and medical applications. More information about the material can be found in the Appendix. A schematic view of the hot embossing process is shown in Fig. 2.

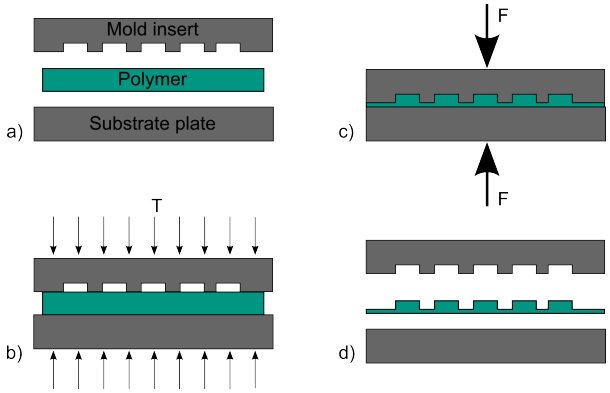

Fig. 2. Schematic view of the hot embossing process. a) A thermoplastic polymer is put between a mold insert and a substrate plate which are each connected to a heating plate. b) The system is closed until a touch force is reached and the system is heated to the molding temperature. c) The molding force is applied and d) after cooling the embossed polymer foil can be demolded.

At the beginning one polymer foil is placed between a mold insert and a substrate plate. Both plates are connected to heating plates to heat them to the molding temperature. The molding temperature is highly dependent on the material and therefore Differential Scanning Calorimetry (DSC) measurements were executed to obtain the thermic properties, like the glass transition temperature, of the polymer foils. After inserting the polymer foil the machine closes until a touch force of 200 N is applied. To improve the molding process the process chamber is then evacuated. Afterwards the system is heated to the molding temperature. When the molding temperature is reached a molding force is applied and the polymer foil is isothermally structured. The molding force is between 60 kN and 120 kN depending on the sturctured area. During cooling the molding force is kept constant until the demolding temperature is reached. After demolding the structured foil can be examined by contact angle measurements.

B. Thermoforming

The structured polymer foils are formed into a three dimensional shape by thermoforming. Fig. 3 shows a schematic view of the thermoforming process. A pre-structured polymer foil is clamped between a mold insert and a counter plate. Both plates are connected to heating plates which heat the inserts and the clamped foil to a temperature below the polymers glass transition temperature. This low temperature is necessary to prevent the destruction of the pre-embossed micro- and nanostructures during the forming process. The clamping force is around 50 kN to assure an airtight sealing of the mold. To improve the forming result an evacuation of the cavities in the mold is done before the forming process. After reaching the forming temperature pressurized gas is inserted with a rate of 0.05 MPa/s. The pressure can be set between 0.05 MPa and 5 MPa. Through the gas pressure the polymer foil is pressed into the cavities. The pressure as well as the clamping force is kept constant during cooling until the demolding temperature is reached.

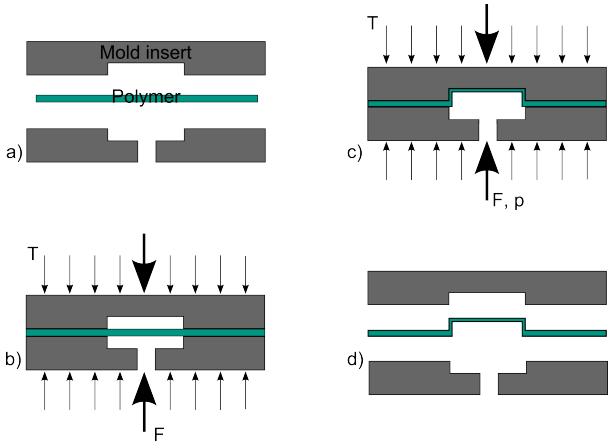

Fig. 3. Schematic view of the thermoforming process. a) A thermoplastic polymer foil is put between a mold insert and a counter plate. b) The system is closed and heated to the forming temperature. A clamping force is applied. c) After reaching the molding temperature the foil is pushed into the cavities of the mold insert by pressurized gas. The pressure is kept constant until the demolding temperature is reached. d) After depressurizing the three dimensional microstructure can be demolded.

C. Bonding

After thermoforming a bonding step is necessary to achieve a closed channel. Therefore the thermoformed foil is bonded to a base plate. The base plate is made out of the same material than the structured foil to facilitate bonding. Different bonding techniques, like thermobonding, ultrasonic bonding and solvent assisted bonding, are known from literature. For first experiments laser welding was used to bond the foil to the base plate.

For Laser welding a diode laser with a wavelength of 940 nm and a maximum power density of 0.38 mW/μm^2 was used. The foil was clamped to the base plate. The material for the base plate was the same as the foil but with a laser-beam absorbent additive. After clamping the laser was scanned over the surface. Thus melting the two polymers at the contact area which lead to a liquid-tight bonding of the two polymers. A schematic view of the laser welding process is shown in Fig. 4.

D. Contact Angle Measurements

For contact angle measurements we used a DataPhysics OC30 contact angle measurement instrument. All experi-

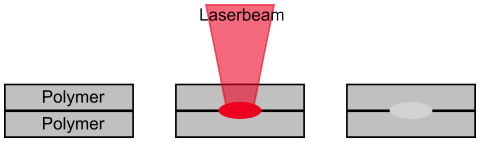

Fig. 4. Schematic view of the laser welding process. Two polymers are a clamped together and melted at the contact area by a laser.

ments were done in a clean room environment with a temperature of 26°C ± 0.8°C and a humidity of 28.5% ± 2.9%. Dynamic and static contact angle measurements were conducted depending on the size of the structured area. For static contact angle measurement a water droplet with a volume of 2 μl was put on the surface. The angle between the surface and the droplet at the triple point was measured and given as the contact angle. Three measurements per sample were taken. For dynamic measurements the "sessile drop needle in" method was used. A droplet was put on the surface with the needle inside. The volume is increased from 1 μl to 10 μl at a rate of 0.2 $\mu l/s$. The volume of 10 μl is halted and when a stable contact angle is reached it is taken as the advancing contact angle. Afterwards the volume is decreased while taking the receding contact angle before the decrease of the base diameter. The contact angle hysteresis is a value for possible contact angles and is calculated as the difference between advancing contact angle and receding contact angle.

III. Results and Discussion

A. Fabrication Process

The hot embossing process step provides the necessary precision to replicate sub-μm structures with high accuracy. Fig. 5 shows two SEM pictures of replicated surfaces.

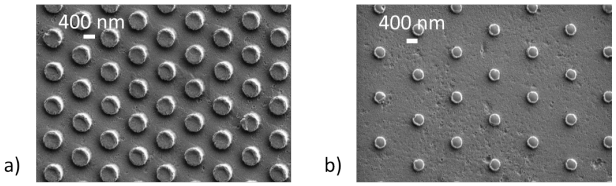

Fig. 5. SEM picture of two hot embossed surfaces. It shows cylindrical pillars with a height of 300 nm and a diameter of a) 750 nm and a pitch of 1500 nm and b) 500 nm and a pitch of 2000 nm from pillar center to center.

After thermoforming and bonding closed liquid-tight channels with inner diameters between 200 μm and 2 mm and micro- and nanostructures on the walls were successfully fabricated as can be seen in Fig. 6. The base plate has the size of a standard glass slide thus enabling an easy use in every microscope. All used materials, PMMA, PC, COC and PSU are transparent and allow the direct observation of biological and medical experiments inside the channel.

B. Contact Angle Measurements

Static contact angle measurements were conducted to examine the influence of pitch and diameter of cylindrical pillars on the contact angle. Fig. 7 shows the used layout of

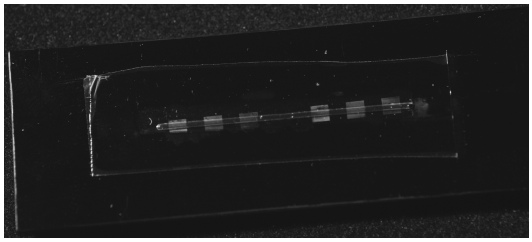

Fig. 6. Picture of a microfluidic chip with a channel with a cross section of 0.5 mm to 0.8 mm and a length of 35 mm. The base plate has the size of a glass slide (26 mm x 76 mm).

the structures. The pitch d is n·Ø with n=2..5. The diameters Ø are 250 nm, 500 nm, 750 nm and 1000 nm.

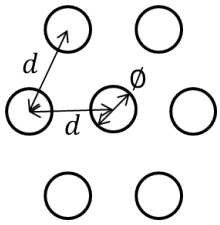

Fig. 7. Schematic view of the structure alignment. The diameters are 250 nm, 500 nm, 750 nm and 1000 nm while the pitch is n·Ø with n=2..5.

Contact angles are widely debated in literature [11]–[15]. Our measurements showed the influence of pitch, diameter and chosen material on the contact angle. With an increase in pitch the contact angle is decreased. The highest decrease can be seen when the pitch increases from 2·Ø to 3·Ø. This agrees with simulations of a material in the Wenzel state. Depending on the material an increase of up to 35° from the unstructured material can be achieved. Because similar results were obtained for all materials only the results of COC are shown in this paper. Fig. 8 shows the contact angle of COC in dependency of pitch and diameter. The error bars are given by the standard deviation. The contact angle is increased with decreasing pitch. For COC an increase of the contact angle from the unstructured contact angle of 85° (mean value of the dynamic contact angle measurements) to 136° was achieved.

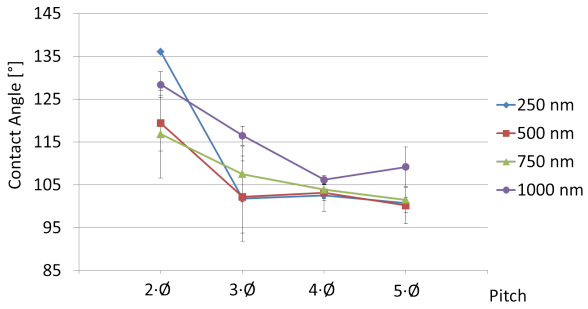

Fig. 8. Change of contact angle of COC in dependency of pitch and diameter. The diameters are 250 nm, 500 nm, 750 nm and 1000 nm while the pitch is n·Ø with n=2..5. The error bars are given by the standard deviation. As a guide for the eye lines were inserted.

To examine the influence of the material on the contact angle, dynamic contact angle measurements were conducted. The foil was structure with cones with a base diameter of 10 μm and a height of 6 μm. Fig. 9 shows the dynamic contact angle of the unstructured material in comparison with a microstructured material for PMMA, PC, PSU and COC. For all materials the contact angle increases by 20°, while the absolute value is dependent of the unstructured materials contact angle.

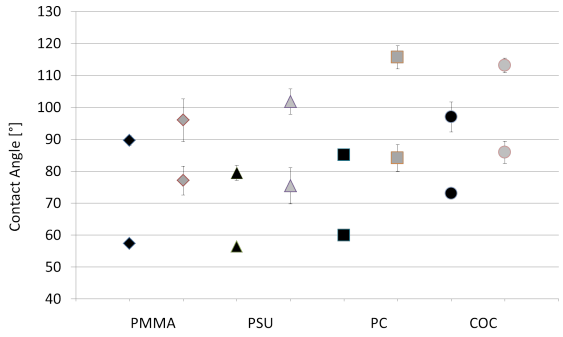

Fig. 9. Comparison of PMMA, PSU, PC and COC. The advancing and receding contact angles of the unstructured (black symbols) and structured material (gray symbols) is shown.

IV. CONCLUSIONS

This work introduced a three step replication process for the fabrication of micro- and nanostructured microfluidic devices. The first step comprises the structuring of the foil by hot embossing. In the next step the form of the microfluidic device is shaped by microthermoforming. In the last step the thermoformed foil is bonded to a base plate with all the necessary fluidic connectors like fluid inlet and outlet. The change of wetting behavior inside the channel is shown by contact angle measurements. An increase of the contact angle by over 40° for Polycarbonate and Cyclic Olefin Copolymer is shown, as well as the dependency of the contact angle from the material and surface structures. We also showed that only by structuring a hydrophilic material can be made hydrophobic. This effect was used for a specific adsorption of BSA. Adsorption experiments showed a specific adsorption on the structured areas. This can be used for biosensors. We also fabricated tubes with structures on the inner and outer surface. Such tubes can be adapted to its application and be used in the medical field like catheters. Also the housing of implants can be structured to improve biocompatibility.

APPENDIX

The following glass transition temperatures T_G were measured at Bürkert GmbH & Co. KG by differential scanning calorimetry (DSC).

Polymethylmethacrylat (PMMA) from Goodfellow, thickness 0.05 mm, T_G= 113°C.

Cyclic Olefin Copolymer (COC), Topas Grade 6013 + 25% elastomeric additives, thickness 0.05 mm, T_G=136.5°C.

Polysulfon (PSU) from Lipp-Terler GmbH, trade name: Lite U, thickness 0.05 mm, T_G=187°C.

Polycarbonate, ordered from it4ip, thickness 0.05 mm, T_G= 149°C.

ACKNOWLEDGMENT

The authors would like to thank P. Abaffy and G. Papagno for capturing the SEM images and Dr. L. Zimmermann and Dipl.-Ing. M. Röhrig for supplying the hot embossing mold inserts. We also thank Dipl-Ing. (FH) H. Besser from the Institute for Applied Materials - Applied Materials Physics (IAM-AWP), KIT for the laser-welding of our microfluidic parts and Ms. Diana Hess from Bürkert GmbH & Co. KG for the differential scanning calorimetry measurements.

REFERENCES

[1] M. Y. H. Nakae, M. Yoshida, "Effects of roughness pitch of surfaces on their wettability," *Journal of Materials Science*, vol. 40, pp. 2287–2293, 2005.

[2] N. Kashaninejad, W. K. Chan, and N. T. Nguyen, "Eccentricity effect of micropatterned surface on contact angle," *Langmuir*, vol. 28, no. 10, pp. 4793–4799, 2012.

[3] S.-H. Yoon, Y. K. Young Kyun Kim, E. D. Han, Y.-H. Seo, B. H. Kime, and M. R. K. Mofrad, "Passive control of cell locomotion using micropatterns: the effect of micropattern geometry on the migratory behavior of adherent cells," *Lab on a Chip*, vol. 12, p. 23912402, 2012.

[4] E. Martinez, E. Engel, J. A. Planell, and J. Samitier, "Effects of artificial micro-and nano-structured surfaces on cell behaviour," *Annals of Anatomy-Anatomischer Anzeiger*, vol. 191, pp. 126–135, 2009.

[5] W. Barthlott and C. Neinhuis, "Purity of the sacred lotus,or escape from contamination in biological surfaces," *Planta*, vol. 202, no. 1, pp. 1–8, 1997.

[6] B. Bhushan and E. K. Her, "Fabrication of superhydrophobic surfaces with high and low adhesion inspired from rose petal," *Langmuir*, vol. 26 (11), pp. 8207–8217, 2010.

[7] M. Worgull, *Hot Embossing: Theory and Technology of Microreplication*, ser. Micro&Nano Technologies. Oxford: William Andrew, 2009.

[8] M. Heilig, M. Schneider, H. Dinglreiter, and M. Worgull, "Technology of microthermoforming of complex three-dimensional parts with multiscale features," *Microsystem Technologies*, vol. 17, pp. 593–600, 2011.

[9] M. Heilig, S. Giselbrecht, A. E. Guber, and M. Worgull, "Microthermoforming of nanostructured polymer films: a new bonding method for the integration of nanostructures in 3-dimensional cavities," *Microsystem Technologies*, vol. 16, pp. 1221–1231, 2010.

[10] R. Truckenmüller, S. Giselbrecht, N. Rivron, E. Eric Gottwald, V. Saile, A. van den Berg, M. Wessling, and C. van Blitterswijk, "Thermoforming of film-based biomedical microdevices," *Advanced Materials*, vol. 23, pp. 1311–1329, 2011.

[11] Y. Y. Yan, N. Gao, and W. Barthlott, "Mimicking natural superhydrophobic surfaces and grasping the wetting process: A review on recent progress in preparing superhydrophobic surfaces," *Advances in colloid and interface science*, vol. 169, no. 2, pp. 80–105, 2011.

[12] X.-M. Li, D. Reinhoudt, and M. Crego-Calama, "What do we need for a superhydrophobic surface? a review on the recent progress in the preparation of superhydrophobic surfaces," *The Royal Society of Chemistry*, vol. 36, pp. 1350–1368, 2007.

[13] T. Young, "An essay on the cohesion of fluids," *Philosophical Transactions of the Royal Society of London*, vol. 95, pp. 65–87, 1805.

[14] R. L. Wenzel, "Resistance of solid surfaces to wetting by water," *Industrial and Engineering Chemistry*, vol. 28, no. 8, pp. 987–994, 1936.

[15] A. Cassie and A. Baxter, "Wettability of porous surfaces," *Transactions of the Faraday Society*, vol. 40, no. 0, pp. 546–551, 1944.